Available online at www.sciencedirect.com
SCIENCE DIRECT®
Earth and Planetary Science Letters 241 (2006) 763–779
EPSL
www.elsevier.com/locate/epsl

# Cenozoic evolution of the sulfur cycle: Insight from oxygen isotopes in marine sulfate

Alexandra V. Turchyn*, Daniel P. Schrag

*Harvard University Department of Earth and Planetary Sciences, 20 Oxford St, Cambridge, MA 02138, United States*

Received 22 May 2005; received in revised form 2 November 2005; accepted 4 November 2005
Available online 20 December 2005
Editor: H. Elderfield

**Abstract**

We report new data on oxygen isotopes in marine sulfate ($\delta^{18}O_{SO4}$), measured in marine barite ($BaSO_4$), over the Cenozoic. The $\delta^{18}O_{SO4}$ varies by 6‰ over the Cenozoic, with major peaks 3, 15, 30 and 55 Ma. The $\delta^{18}O_{SO4}$ does not co-vary with the $\delta^{34}S_{SO4}$, emphasizing that different processes control the oxygen and sulfur isotopic composition of sulfate. This indicates that temporal changes in the $\delta^{18}O_{SO4}$ over the Cenozoic must reflect changes in the isotopic fractionation associated with the sulfide reoxidation pathway. This suggests that variations in the aerial extent of different types of organic-rich sediments may have a significant impact on the biogeochemical sulfur cycle and emphasizes that the sulfur cycle is less sensitive to net organic carbon burial than to changes in the conditions of that organic carbon burial. The $\delta^{18}O_{SO4}$ also does not co-vary with the $\delta^{18}O$ measured in benthic foraminifera, emphasizing that oxygen isotopes in water and sulfate remain out of equilibrium over the lifetime of sulfate in the ocean. A simple box model was used to explore dynamics of the marine sulfur cycle with respect to both oxygen and sulfur isotopes over the Cenozoic. We interpret variability in the $\delta^{18}O_{SO4}$ to reflect changes in the aerial distribution of conditions within organic-rich sediments, from periods with more localized, organic-rich sediments, to periods with more diffuse organic carbon burial. While these changes may not impact the net organic carbon burial, they will greatly affect the way that sulfur is processed within organic-rich sediments, impacting the sulfide reoxidation pathway and thus the $\delta^{18}O_{SO4}$. Our qualitative interpretation of the record suggests that sulfate concentrations were probably lower earlier in the Cenozoic.


*Keywords:* sulfate; oxygen isotopes; Cenozoic; carbon cycle; sulfur cycle; coupled biogeochemical cycles; barite

## 1. Introduction

Marine sulfate plays an important role in biogeochemical cycling in organic-rich sediments, serving as the terminal electron acceptor in the remineralization of organic matter and responsible for nearly all anaerobic methane oxidation [1,2]. The majority of studies of the sulfur cycle have focused on sulfur isotopes, whose temporal variations are interpreted to reflect changes in net sulfide burial and sulfide weathering [3]. However, sulfur isotopes are conserved during sulfate reduction and sulfide reoxidation in organic-rich sediments. Recent work has suggested that the sulfate cycle may have varied considerably more through Earth history than was previously assumed due to the importance of this sulfur cycling in organic-rich sediments [4].

* Corresponding author. Currently at the Department of Earth and Planetary Sciences, UC Berkeley, McCone Hall, Berkeley, CA 94720, United States.
*E-mail address:* avturchyn@berkeley.edu (A.V. Turchyn).

0012-821X/$ - see front matter © 2005 Elsevier B.V. All rights reserved.
doi:10.1016/j.epsl.2005.11.007

The biogeochemical sulfur cycle is controlled by input from rivers, sulfate reduction and reoxidation on continental shelves and slopes (which controls the burial of sedimentary pyrite and organic sulfur), and permanent burial of sulfate in the ocean crust during hydrothermal circulation as anhydrite and pyrite. The sulfate fluxes from reduction and oxidation on continental shelves and slopes dominate the sulfate budget in the modern ocean, with sulfate reduction rates ranging from 2 to 10 mol/m$^2$/yr in the shallowest continental shelf environments [5,6] to 0.002 to 0.1 mol/m$^2$/yr on the continental slope [1,7–12]. Although in the presence of reactive iron oxides sulfide can react and form metastable iron sulfides, the majority of the sulfide produced during sulfate reduction in the modern ocean is reoxidized at the sediment–water interface; sulfide reoxidation rates range between 75% and 90% of sulfate reduction rates [5,7]. Given the global extent of ocean area where this reduction and reoxidation occurs, these fluxes are between two and three times the river flux (which is 2 to $3.5\times10^{12}$ mol/yr—[13,14]). Most previous studies of seawater sulfate assume a long residence time ($>10^7$ yr) based solely on river input. However, because of the high rates of sulfate reduction and sulfide reoxidation, the effective residence time for oxygen isotopes in marine sulfate is closer to 1 Ma [4]. In hydrothermal systems, sulfate may also be buried in the crust as anhydrite or pyrite, the magnitude of this sink has been estimated from 0.5 to $4.1\times10^{12}$ mol/yr [14–16]. In addition to these major sources and sinks of sulfate in the ocean, smaller fluxes are sulfate associated carbonate precipitation ($0.15\times10^{12}$ mol/yr, [17]), serpentization of the ocean crust (0.01 to $0.2\times10^{12}$ mol/yr, [18]), volcanic input (0.18 to $0.3\times10^{12}$ mol/yr — [19,20]), evaporite formation (0.1 to $0.4\times10^{12}$ mol/yr, [21]) and dimethyl sulfide oxidation ($0.7\times10^{12}$ mol/yr [22]).

Oxygen is continually incorporated into the sulfur cycle through the oxidation of sulfides to sulfate then released through sulfate reduction. The $\delta^{18}$O of sulfate ($\delta^{18}O_{SO4}$) in the modern ocean has been measured at 9.3‰ [23]). At ocean temperature and pH, oxygen isotopes between sulfate and water should not equilibrate within 10 Ma [24]. Sulfate reduction preferentially reduces sulfate with lighter oxygen isotopes, but sulfate–enzyme coupling also allows isotopic exchange between sulfate and water during reduction, leaving the residual sulfate pool initially 8‰ to 10‰ enriched over seawater, and up to 25‰ enriched in sulfate limited environments [25]. There are three known pathways of sulfide reoxidation on continental shelves. First, bacterial disproportionation reactions (during which $H_2S$ and $SO_4^{2-}$ are simultaneously produced) produces sulfate which is enriched by 8‰ to 17‰ over the $\delta^{18}$O of the ocean ($\delta^{18}O_{sw}$), depending on the metal oxide present [26,27]. Second, direct sulfide oxidation produces sulfate which has approximately the same isotopic composition as the water in which it was oxidized [28]. Finally, biological oxidation of sulfide, which typically proceeds through the intermediate sulfite ($SO_3^{2-}$), produces sulfate which is 20–25‰ enriched over the water in which it was oxidized [28]. Direct sulfide oxidation is believed to dominate in oxic, well bioturbated sediments, whereas the biological reoxidation pathways are believed to dominate in low-oxygen bottom waters where sulfur bacteria thrive [28].

Studies of paleovariations in sulfur and strontium isotopes have often relied on marine barite as the mineral phase [29–31]. Barite precipitates in the water column when surface dwelling plankton are consumed by zooplankton, creating microenvironments where barite is supersaturated and precipitates [32]. These plankton concentrate barium in their shells and in their organic matter and thus their decay in the presence of sulfate creates the supersaturated conditions necessary for barite precipitation [32]. Acantharia, surface dwelling protists that make their shells out of strontium sulfate (celestite) may be particularly important in marine barite precipitation [33]. Another possible source of barite to pelagic sediments is the Xenophyophorea, benthic protists that form barite exoskeletons, which may be agglutinated from falling barite crystals in the ocean biomineralizes [34]. Barite offers advantages over other sulfate minerals for studying paleo-$\delta^{18}O_{SO4}$ because of its resistance to diagenesis in pelagic sediments and the uninterrupted record not afforded by sulfate evaporite deposits [29].

In this paper we explore temporal changes in the marine sulfate cycle through the analysis of $\delta^{18}$O of marine barite ($BaSO_4$) over the Cenozoic. Temporal variations in $\delta^{18}O_{SO4}$ are compared to variations in $\delta^{34}S_{SO4}$ and $\delta^{13}$C to better understand the processes driving changes in the oxygen isotopic composition of sulfate. A simple box model will be used to explore the dynamics of the sulfur cycle.

## 2. Methods

### 2.1. Analytical methods

Pelagic sediments were selected from ODP and DSDP sites in the tropical Pacific Ocean. Sites were selected based on regions with previous success in extracting usable amounts of trace barite [29,30]. Age models were recalculated using biostratigraphic controls

provided by E. Thomas (personal communication). Barite was extracted from sediments using a method designed to reduce oxygen isotope exchange between sulfate and water. Earlier experiments have demonstrated that oxygen isotopes in sulfate equilibrate with water at high temperature and/or low pH [23,24]. Preliminary analysis of barite extracted through a high temperature acidic preparation [29,30] showed large variability in $\delta^{18}O$, suggesting a gravimetric approach to silicate removal, with only weak acids used to dissolve carbonates.

Sediment was dispersed in deionized water then repeatedly digested in 1 M Acetic Acid (pH ≈ 3) to dissolve carbonate minerals. The remaining sediment was repeatedly rinsed with deionized water, then dried, manually ground to powder, and sieved to 200 μm. The powder was suspended in a 2.85 g/cc Lithium Polytungstate (LST) solution to separate barite, which has high density (4.5 g/cm$^3$), from clays. All higher density material was extracted and rinsed. To oxidize any residual organic matter, the remaining material remained for several days in sodium hypochlorite warmed to 50 °C. Following the oxidation step, the residue was rinsed and heated to 80 °C with 1 N NaOH to dissolve opal (typically diatom frustules). Occasionally barite crystals were found embedded in diatom frustules, possibly from the grinding, which resulted in opal settling with the heavy fraction. After this base dissolution, the residue was rinsed and placed in a 0.02 M hydroxylamine hydrochlorite in 10 vol.% acetic acid to clear the barite of any transition metal-oxyhydroxides. The final step was to place the barite in a 6 N HCl solution for 10 min to dissolve acid soluble minerals, such as apatite and colloidal iron oxides. Finally, the samples were thoroughly rinsed and the purity was measured through viewing on a Scanning Electron Microscope (SEM) with energy dispersive X-ray spectroscopy (EDX) capability. If SEM images or EDX backscatter patterns indicated minerals other than barite (silicates, tungstates, iron oxides) the samples were resuspended and re-extracted. In addition, X-ray diffraction (XRD) patterns were run on over half the samples.

Samples containing high density clays were resuspended in LST and heated to 40 °C; at this temperature the density of the LST solution increased to 3.1 g/cm$^3$. The clay minerals were removed as they migrated to the top of the solution. Samples containing calcium tungstate precipitates (e.g. scheelite) were discarded and reextracted because tungstates are difficult to dissolve without using concentrated acids at elevated temperatures for an extended period of time. Tungstate precipitates were formed in some samples when a different heavy liquid, Sodium Polytungstate — SPT was used, but were not encountered using LST. Any samples that still contained non-barite XRD lines or images of non-barite crystals were discarded. It is estimated that the samples run for oxygen isotope analysis were >90% pure.

Samples were analyzed for their oxygen isotopic composition through pyrolysis in a graphite crucible in a Temperature Conversion Element Analyzer (TC/EA) at 1450 °C coupled by continuous He flow to a Delta Plus mass spectrometer, where oxygen isotopes were measured as carbon monoxide (CO). The standard used to make the $\delta^{18}O$ measurement was Vienna Standard Mean Ocean Water (V-SMOW). Repeated measurements of a barite standard (NBS/NIST-127) were made. This standard has several reported values in the literature; 9.8‰ [23], 9.3–9.4‰ (NIST Website and materials) and 8.6‰ [35]. Measurements using our technique yielded values of 9.73 ± 0.42‰ (2$\sigma$ standard deviation). An additional standard, EM Barite, was sieved, measured, and found to have a value of 14.46 ± 0.54‰ (2$\sigma$ standard deviation). Both standards were measured several times during each sample run, allowing for both drift correction and internal verification (NIST and EM standards were expected to maintain a 4.5–5.0‰ difference). All extracted barite samples were corrected to NIST-127 value of 9.3‰. Measurement precision and accuracy were greatly enhanced by adding 2–4 mg of platinum powder to each sample. We believe that the platinum helps both catalyze and normalize the formation of CO in the reactor.

### 2.2. Modeling methods

To model the sulfur cycle we use conservation equations for sulfate:

$$\partial(M_{SO4})/dt = J_{rivers} + f^{*}J_{reduc} - J_{reduc} - J_{alteration} \quad (1)$$

| | |
|---|---|
| $M_{SO4}$ | the amount of sulfate in the ocean (mol) |
| $J_{rivers}$ | the flux of sulfate from rivers (mol/yr) |
| $J_{reduc}$ | the sulfate reduction rate (mol/yr) |
| $f$ | the fraction of sulfide produced from sulfate reduction which is subsequently reoxidized |
| $f^{*}J_{reduc}$ | is the shelf and slope sulfide reoxidation rate |
| $J_{alteration}$ | the sink term associated with the precipitation of anhydrite and pyrite in hydrothermal systems |

And for $\delta^{18}O_{SO4}$:

$$\begin{aligned}\partial\left(\delta^{18}O_{SO4}M_{SO4}\right)/dt = {} & J_{rivers}\left(\delta^{18}O_{SO4-riv}\right) \\ & + f^{*}J_{reduc}\left(\varepsilon_x - \delta^{18}O_{SO4}\right) \\ & - J_{reduc}\left(\delta^{18}O_{SO4} - \varepsilon_y\right) \\ & - J_{alteration}\left(\delta^{18}O_{SO4}\right) \end{aligned} \quad (2)$$

$\delta^{18}O_{SO4}$ is the oxygen isotopic composition of marine sulfate
$\delta^{18}O_{SW}$ is the oxygen isotopic composition of the ocean
$\delta^{18}O_{SO4\text{-}riv}$ is the oxygen isotopic composition of riverine sulfate
$\varepsilon_x$ is the isotopic fractionation associated with sulfide reoxidation
$\varepsilon_y$ is the isotopic fractionation associated with the selection for light sulfate during sulfate reduction.

To initialize the model for the modern ocean, we take the mass of sulfate as $3.78 \times 10^{19}$ mol and the sulfate flux from rivers as $3.0 \times 10^{12}$ mol/yr [13,14,36]. Sulfate reduction rates were modeled as an exponential curve decreasing from 4 mol/m$^2$ yr at 1 m water depth to 0.0001 mol/m$^2$ yr at 2000 m (based on a compilation of data shown in Fig. 1) and reoxidation rates are expressed as a percentage of the reduction rates [5,7,11]. Sulfate reduction rates in the deep ocean are several orders of magnitude less than those on the continental slopes and shelves [37] and were neglected. These calculations suggest the average continental shelf reduction rate is 3.3 mol/m$^2$ yr with 84% reoxidized (to 150 m water depth) and average continental slope reduction rates of 0.5 mol/m$^2$ yr with 77% reoxidized (150–2000 m water depth). The magnitude of $J_{reduc}$ will depend on the area in the ocean where these rates occur. We assume that at any given water depth approximately 10% of the available ocean classifies as "high productivity," which accounts for areas of the ocean which are not highly productive and thus do not have significant rates of sulfate reduction. Summing these modeled rates over this modified area yields a total modern ocean sulfate reduction rate of $7.7 \times 10^{12}$ mol/yr. With 83% reoxidized, a pyrite deposition rate of $1.3 \times 10^{12}$ mol/yr is suggested, which is 40% of the river input, similar to previous estimates (~35%, [36]). Using organic carbon burial rates, independent measurements of sedimentary pyrite deposition estimate $1.2 \times 10^{12}$ mol/yr [38], which further validates our calculations.

Balancing the sulfate budget yields a modern ocean value for $J_{alteration}$ of $1.65 \times 10^{12}$ mol/yr. The magnitude of sulfide burial in hydrothermal systems has been estimated at 0.5 to $0.8 \times 10^{12}$ mol/yr [39]. The amount sulfate permanently buried in the crust as anhydrite is uncertain, because most of it is thought to dissolve off axis. Various calculations suggest this sink is between 1 and $4 \times 10^{12}$ mol/yr [14–16,36]. Our calculated value of $1.65 \times 10^{12}$ mol/yr is in the range of these values, corroborating our calculations.

Evaporite formation is often considered as major, if episodic sink, in the marine sulfur cycle (e.g. [41]). Even during times in Earth history with large evaporite basins, the rate of formation is small compared with the major fluxes listed above. For example, during the Messinian salinity crisis 6 Ma, when widespread evaporite formation occurred in much of the Mediterranean and Persian Gulf, the estimated evaporite deposition rate was $0.25 \times 10^{12}$ mol/yr (calculated from [21]). We have not included evaporite deposition in our model.

River $\delta^{18}O_{SO4}$ can vary greatly due to local mineralogy [40]. Weathering of sulfate evaporites (average isotopic composition of +11‰ to +13‰, [41]), will drive river $\delta^{18}O_{SO4}$ more positive, while weathering of sulfide deposits produces sulfate with a $\delta^{18}O_{SO4}$ between −4‰ and +2‰ [42]. Anthropogenic sulfate

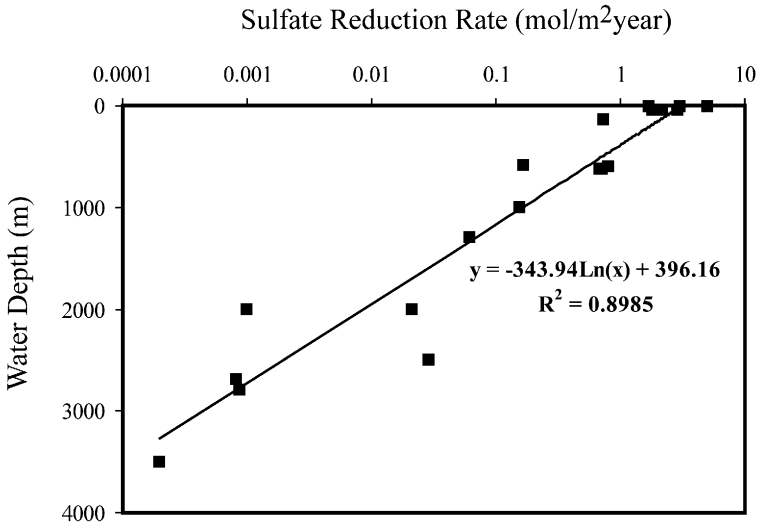


Fig. 1. A compilation of literature reported sulfate reduction rates in mol/m$^2$ yr, showing an exponential decrease with increasing water depth. Data taken from Niewöhner et al. [1], Canfield [7], D'Hondt et al. [37], Thamdrup et al. [8], Huang and Lin [9], Borowski et al. [10], Lin and Morse [11], and Aharon and Fu [12].

Table 1
Values used in the model

| Description | Term | Value | Unit |
|---|---|---|---|
| Mass of sulfate in the ocean | $M_{SO4}$ | $3.78\times10^{19}$ | Mol/yr |
| Flux of sulfate from rivers | $J_{rivers}$ | $3\times10^{12}$ | Mol/yr |
| Sulfate reduction rates | $J_{reduc}$ | $8\times10^{12}$ | Mol/yr* |
| Sulfide reoxidation rate | $f^*J_{reduc}$ | 83 | % of $J_{reduc}$ |
| Burial flux | $J_{burial}$ | $2\times10^{12}$ | Mol/yr** |
| Oxygen isotopes in river sulfate | $\delta^{18}O_{SO4\text{-}riv}$ | 4 | ‰ |
| Fractionation during sulfate reduction | $\varepsilon_y$ | 2 to 14 (7) | ‰ |
| Fractionation during reoxidation | $\varepsilon_x$ | 2 to 20 (9 to 17) | ‰ |

* Varies as a function of sulfate concentration and shelf area.
** Varies as a function of sulfate concentration.

will drive the riverine $\delta^{18}O_{SO4}$ as high as 40‰ therefore natural riverine $\delta^{18}O_{SO4}$ must be estimated [40]. A 2:1 ratio in rivers of sulfate from evaporite versus pyrite weathering [36] yields a calculated $\delta^{18}O_{SO4}$ for rivers of +5.4‰ to +7.0‰. Independent compilations of surface runoff data corrected for anthropogenic influence by [28] show riverine sulfate ranging between −2‰ and +5‰. The value for $\delta^{18}O_{SO4\text{-}riv}$ used in Eq. (2) is 4‰.

During bacterial sulfate reduction, sulfate with lighter oxygen isotopes is preferentially reduced, leaving a residual sulfate pool that is enriched in $\delta^{18}O_{SO4}$. Oxygen isotope exchange through sulfate–enzyme coupling during dissimilatory sulfate reduction causes the $\delta^{18}O_{SO4}$ of the residual sulfate pool eventually to approach a single isotopic value, 25–30‰ enriched above $\delta^{18}O_{SW}$ in sulfate limited environments [25,28]. The control on the magnitude of oxygen isotope fractionation during sulfate reduction ($\varepsilon_o$) is not well constrained but, like sulfur isotopes, may be related to the type of carbon used as an electron donor (e.g. [12,41]). Measurements of oxygen isotopes in sulfate porewater profiles suggest that $_o$ can be 2‰ to 10‰ [12]. We use a value of 7‰ for $_y$ in Eq. (2), although we have allowed this to vary between 2‰ and 14‰.

Reoxidation of sulfide to sulfate produces a variety of isotopic values for the resulting sulfate, depending on the reoxidation pathway. Disproportionation reactions produce sulfate which is on average 15‰ enriched over sea water, depending on the relative availability of iron and manganese (manganese produces $\delta^{18}O_{SO4}$ 8‰ to 12‰ enriched over $\delta^{18}O_{SW}$ while iron produces $\delta^{18}O_{SO4}$ 17‰ enriched over $\delta^{18}O_{SW}$ — [26,27]. Direct sulfide oxidation produces sulfate with $\delta^{18}O_{SO4}$ that is approximately equal to the water in which it was oxidized. Sulfur intermediates, particularly sulfite ($SO_3^{2-}$) can rapidly isotopically equilibrate with water, enriching the sulfite in $^{18}O$ by as much as 23‰. The sulfate resulting from oxidation through sulfite will thus be highly isotopically enriched, up to 20‰ over the water in which it was oxidized [28]. We could allow $\varepsilon_x$ to vary from 2‰ to 20‰, although we kept it between 9 and 17‰. All the fluxes and isotopic values used in Eq. (2) are summarized in Table 1.

Eq. (2) was solved both for steady state and using finite difference (time step 10,000 yr) to explore temporal changes in the sulfate system. Eqs. (1) and (2) are coupled such that $J_{alteration}$ is a function of the amount of sulfate in the ocean and $J_{reduc}$ is a function of both the amount of sulfate in the ocean and the shelf area. This allows us to simultaneously monitor changes in the sulfate concentration and its isotopic composition.

Sea level fluctuations, which cause the subaereal exposure of the shelves, impact the marine sulfate cycle by reducing sulfate reduction and sulfide reoxidation and increasing pyrite weathering on the exposed continental shelves (producing isotopically light sulfate). A term was added to Eqs. (1) and (2) to account for pyrite weathering on exposed continental shelves at low sea level by breaking the shelves into boxes of equal area every 10 m water depth, such that when sea level rose or fell 10 m, a fixed amount of shelf area would become submerged or exposed. A schematic of this is shown in Fig. 2. For each box of continental shelf exposed, we applied oxidative pyrite weathering rates from experimental work at neutral pH [44]. This weathering also accounts for the influence of changes in the isotopic composition of meteoric water on the marine sulfate cycle, including the increasing importance of groundwater weathering at low sea level.

Sulfur isotopes in marine sulfate can be modeled using a single conservation equation coupled to those for oxygen isotopes in order to simultaneously model changes in $\delta^{34}S_{SO4}$ and $\delta^{18}O_{SO4}$:

$$d\left(\delta^{34}S_{SO4t+1}M_{SO4}\right)/dt = J_{rivers}\left(\delta^{34}S_{SO4-riv}\right) - \left(J_{reduc} - f^*J_{reduc}\right) *\left(\delta^{34}S_{SO4} - \varepsilon_S\right) - J_{alteration}\left(\delta^{34}S_{SO4}\right) \quad (2)$$

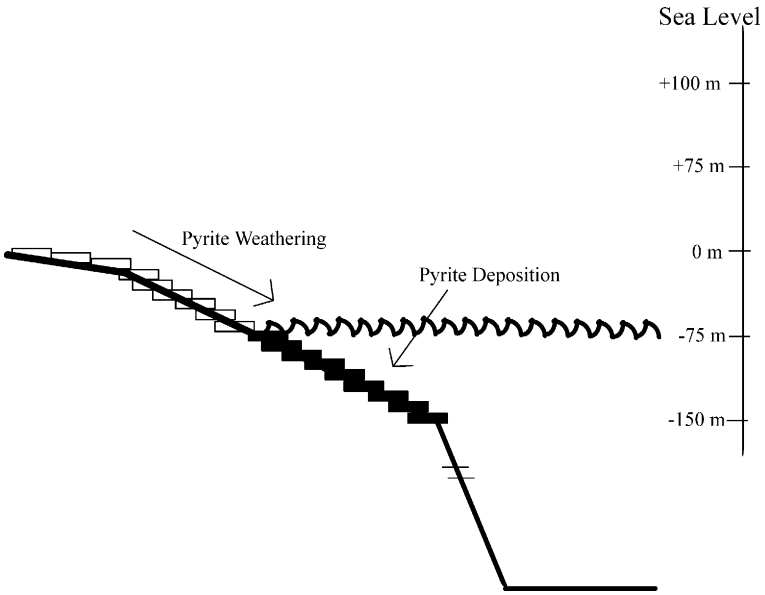


Fig. 2. A schematic drawing of how sea level variations were incorporated into our model of the sulfate cycle. The boxes on the continental shelf each represent 10 m water depth. Dark boxes show areas of pyrite deposition where empty boxes show subaereally exposed shelf from which occurs net pyrite weathering. The drawing is not to scale. Refer to text for details.

where

$\delta^{34}S_{SO4}$ is the sulfur isotopic composition of sulfate in the oceans,
$\delta^{34}S_{SO4-riv}$ is the sulfur isotopic composition of sulfate in rivers (10‰ — [30])
$J_{reduc} - f^* J_{reduc}$ is the difference between sulfate reduction and sulfide reoxidation, which represents pyrite burial
And $\varepsilon_S$ is the sulfur isotope fractionation between sulfate and pyrite (10–60‰, depending on the dominant microbial community and the type of carbon substrate available — [43]).

## 3. Results

A plot of $\delta^{18}O_{SO4}$ in marine barite over the Cenozoic is shown in Fig. 3. The $\delta^{18}O_{SO4}$ of marine barite begins the Cenozoic increasing from 9‰ to 14‰, which it reaches around 55 Million years ago (Ma), at the Paleocene/Eocene boundary. After this peak it declines by 4‰ over the next 15 Myr. There is too much variability in the data to be able to resolve shorter term variations in the record over this period of time. After the nadir between 35 and 40 Ma, the $\delta^{18}O_{SO4}$ increases by 2‰ over the next 5 Myr, then decreases by 1‰ from 30 to 20 Ma, followed by an increase to 14‰ at 15 Ma. After this peak the $\delta^{18}O_{SO4}$ declines to 9‰ over the next 8 Myr. Then the $\delta^{18}O_{SO4}$ increases back to 14‰, after which there is an abrupt decline of 5‰ over the last 3 Myr. Overall, the $\delta^{18}O_{SO4}$ appears cyclical over the Cenozoic. This is particularly evident after the Eocene/Oligocene boundary when three distinct cycles begin, increasing in period and amplitude to the modern. This trend is reproduced among ten sites drilled in the different DSDP and ODP legs.

The $\delta^{18}O_{SO4}$ record in marine barite over the Cenozoic is also compared with the $\delta^{18}O$ in benthic foraminifera record ([45]—Fig. 4c), the $\delta^{34}S_{SO4}$ record in marine barite ([30]—Fig. 4d) and with the $\delta^{13}C$ in benthic foraminifera record ([45]—Fig. 4b). The $\delta^{18}O_{SO4}$ shows little correlation with the $\delta^{18}O$ in benthic foraminifera (Fig. 4a,c), demonstrating that sulfate and water remained out of isotopic equilibrium. The $\delta^{18}O_{SO4}$ also shows little correlation with sulfur isotope variations in marine sulfate (Fig. 4a,d), suggesting that different processes control the isotopic composition of the oxygen and sulfur atoms in sulfate. The peak in $\delta^{18}O_{SO4}$ 15 Ma appears roughly coincident with a similar peak in the $\delta^{13}C$ in benthic foraminifera attributed to the Mid-Miocene Climate Optimum (Fig. 4a,b).

## 4. Discussion

### 4.1. Potential concerns about the data

Modern marine barite (7.9‰) does not have the same $\delta^{18}O_{SO4}$ as seawater sulfate (9.3‰), which could be due to an isotopic fractionation during barite precipitation or an isotopic fractionation during pyrolysis in the TC/EA. Studies of the $\delta^{34}S$ and strontium isotopes in marine barite found no fractionation be-

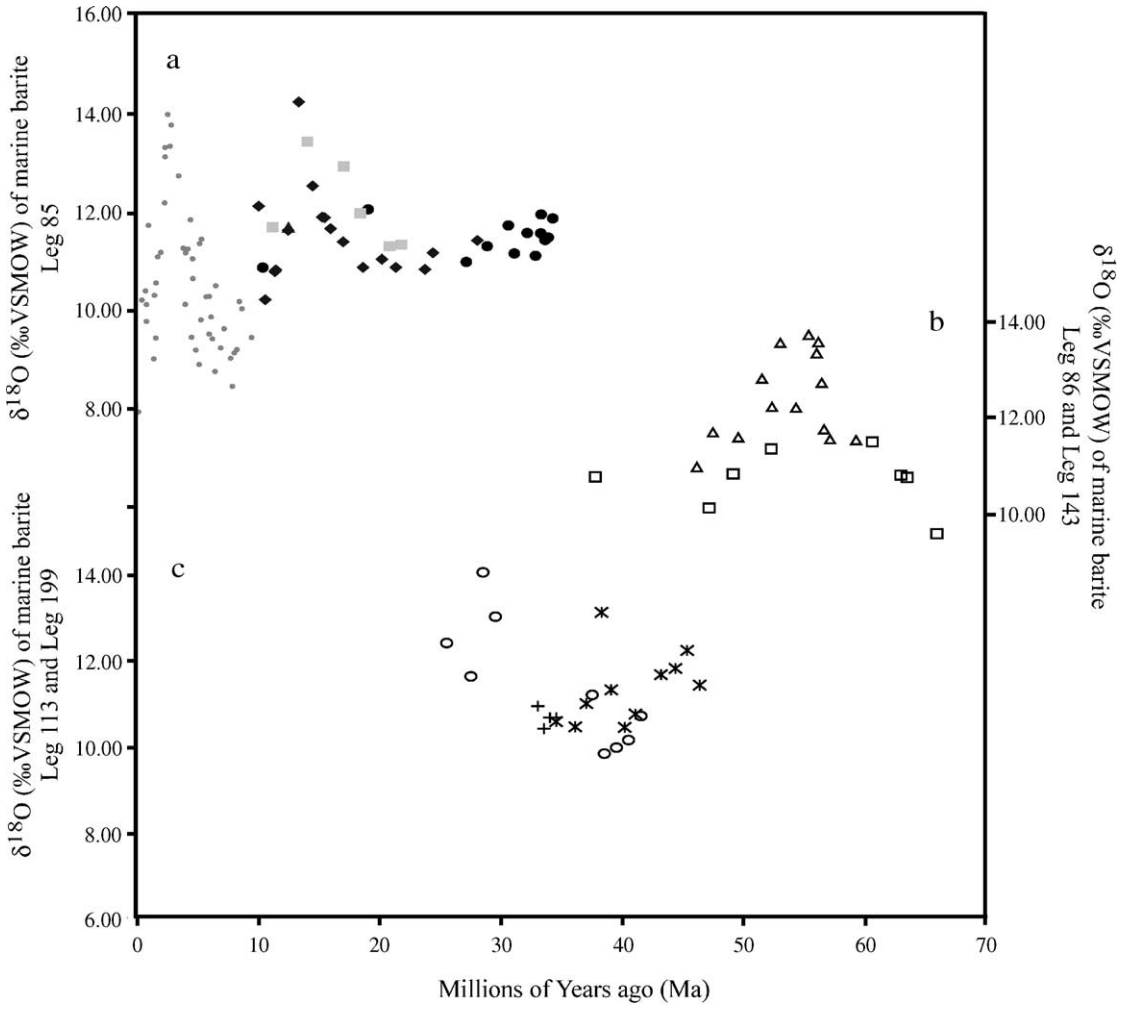


Fig. 3. Data from this study separated into three blocks. (a) The $\delta^{18}O_{SO4}$ of marine barite extracted from Leg 85, data from 0–10 Ma are from Turchyn and Schrag [4]. Data points are: filled triangles: DSDP 572, filled circles: DSDP 573, filled diamonds: DSDP 574, filled squares: DSDP 575. (b) The $\delta^{18}O_{SO4}$ of marine barite extracted from Legs 86 and 143, open squares: DSDP 577, open triangles: ODP 865. (c) The $\delta^{18}O_{SO4}$ of marine barite extracted from Legs 113 and 199; + signs: DSDP 689, open circles: ODP 1218, *: ODP 1219. The data are plot in separate blocks to examine how the various sites compare with one another. Standard deviations for each data point are presented in Table 2.

tween marine sulfate and marine barite [29,30]; however, the crystal structure of barite–the barium atoms bind directly to the oxygen atoms–suggests the possibility of a preference among oxygen isotopes during barite formation. Although our measurement technique is new, repeated measurements of NIST 127 (9.73 ± 0.42‰) indicate that the analytical method is sufficiently accurate for the magnitude of the variations that we observe. We propose that the 1.4‰ fractionation between sulfate and barite is a kinetic isotopic effect associated with barite precipitation and that it is independent of temperature at low temperatures (similar to other sulfate mineral systems—[41]).

Another concern is that the marine barite samples have undergone diagenesis. Diagenesis affects barite in sediment where porewater sulfate concentrations are reduced to zero. In these conditions, barite dissolves, the sulfate is reduced, and barite reprecipitates at the oxic/anoxic interface. Diagenetic barite should have anomalously high $\delta^{18}O_{SO4}$. This has been confirmed by measurements of purely diagenetic samples in our lab which had a $\delta^{18}O_{SO4}$ between 20‰ and 23‰. In addition, diagenetic barite is readily identified in SEM images because the crystals are larger and have a pitted, block-like morphology [31]. It is unlikely that at 3500 m water depth, the minimum depth of the sites where we extracted samples, there were significant rates sulfate reduction over the Cenozoic. Estimates of sulfate reduction rates in these water depths are close to 5 orders of magnitude less than those on the

Table 2
Measurements of the $\delta^{18}O$ of marine barite over the Cenozoic

| Leg-Site-Core-Section | # Run | Age | $\delta^{18}O$ (‰ VSMOW) | Standard deviation i($1\sigma$) |
|---|---|---|---|---|
| 85-572D-13-5 | 3 | 11.75 | 13.39 | 0.23 |
| 85-573B-14-5 | 3 | 17.85 | 12.41 | 0.69 |
| 85-573B-24-2 | 1 | 25.10 | 11.73 | 0.00 |
| 85-573B-24-4 | 3 | 25.37 | 10.98 | 0.07 |
| 85-573B-27-1 | 3 | 26.95 | 11.80 | 0.10 |
| 85-573B-28-3 | 3 | 29.04 | 12.05 | 0.15 |
| 85-573B-29-4 | 1 | 29.90 | 11.96 | 0.00 |
| 85-573B-29-5 | 2 | 30.03 | 11.58 | 0.11 |
| 85-573B-32-1 | 3 | 30.65 | 11.11 | 0.66 |
| 85-573B-33-3 | 2 | 31.07 | 11.58 | 0.28 |
| 85-573B-34-1 | 2 | 31.39 | 11.44 | 0.04 |
| 85-573B-35-5 | 2 | 31.62 | 11.49 | 0.06 |
| 85-573B-37-1 | 2 | 31.99 | 11.88 | 0.03 |
| 85-573B-4-3 | 9 | 9.79 | 10.66 | 0.33 |
| 85-574-10-3 | 10 | 10.78 | 10.22 | 0.22 |
| 85-574-20-5 | 4 | 14.34 | 14.25 | 0.38 |
| 85-574-22-2 | 3 | 14.97 | 11.99 | 0.08 |
| 85-574-8-6 | 7 | 9.46 | 11.23 | 0.75 |
| 85-574-9-3 | 7 | 9.97 | 12.10 | 0.67 |
| 85-574A-10-2 | 6 | 10.71 | 12.13 | 0.31 |
| 85-574A-11-4 | 4 | 11.72 | 10.79 | 0.12 |
| 85-574A-15-2 | 1 | 12.54 | 14.91 | 0.00 |
| 85-574A-19-3 | 1 | 13.61 | 12.55 | 0.00 |
| 85-574A-21-1 | 2 | 14.51 | 12.93 | 0.44 |
| 85-574B-1-6 | 2 | 15.94 | 11.90 | 0.70 |
| 85-574C-10-4 | 1 | 19.97 | 10.88 | 0.00 |
| 85-574C-14-2 | 3 | 22.20 | 11.04 | 0.47 |
| 85-574C-16-3 | 3 | 22.80 | 11.83 | 0.79 |
| 85-574C-20-1 | 1 | 26.20 | 10.84 | 0.00 |
| 85-574C-20-6 | 1 | 26.81 | 10.94 | 0.00 |
| 85-574C-27-3 | 1 | 30.97 | 11.76 | 0.00 |
| 85-574C-4-2 | 2 | 17.44 | 11.70 | 0.87 |
| 85-574C-7-4 | 2 | 18.89 | 10.79 | 0.25 |
| 85-575-5-4 | 1 | 10.56 | 11.69 | 0.00 |
| 85-575-8-3 | 6 | 13.21 | 13.48 | 0.41 |
| 85-575A-20-3 | 1 | 17.25 | 12.80 | 0.00 |
| 85-575A-25-3 | 1 | 19.48 | 12.31 | 0.00 |
| 85-575A-31-2 | 1 | 20.38 | 11.34 | 0.00 |
| 85-575A-5-2 | 1 | 15.97 | 12.93 | 0.00 |
| 86-577-8-1 | 4 | 37.71 | 10.77 | 0.35 |
| 86-577-8-5 | 2 | 47.02 | 10.13 | 0.04 |
| 85-577-8-6 | 2 | 48.99 | 10.84 | 0.16 |
| 85-577-9-2 | 3 | 52.10 | 11.38 | 0.14 |
| 86-577-11-5 | 1 | 60.37 | 11.49 | 0.00 |
| 86-577-12-2 | 3 | 62.75 | 10.80 | 0.25 |
| 86-577-12-3 | 2 | 63.26 | 10.76 | 0.13 |
| 86-577-13-2 | 1 | 65.69 | 9.61 | 0.00 |
| 113-689B-13-3 | 3 | 33.9 | 10.93 | 0.35 |
| 113-689B-13-5 | 3 | 34.1 | 10.41 | 0.67 |
| 113-689B-14-3a | 3 | 34.3 | 10.66 | 0.65 |
| 113-689B-14-3b | 3 | 34.3 | 10.67 | 0.47 |
| 143-865B-10-3 | 3 | 52.17 | 12.22 | 0.12 |
| 143-865B-10-5 | 3 | 52.84 | 13.54 | 0.92 |
| 143-865B-11-3 | 3 | 54.13 | 12.21 | 0.59 |
| 143-865B-11-5 | 3 | 55.18 | 13.71 | 0.20 |
| 143-865B-12-4 | 3 | 55.83 | 13.33 | 0.09 |
| 143-865B-12-6 | 3 | 55.97 | 13.56 | 0.25 |

Table 2 (*continued*)

| Leg-Site-Core-Section | # Run | Age | $\delta^{18}O$ (‰ VSMOW) | Standard deviation ($1\sigma$) |
|---|---|---|---|---|
| 143-865B-13-1 | 3 | 56.22 | 12.72 | 0.23 |
| 143-865B-13-2 | 3 | 56.43 | 11.76 | 0.23 |
| 143-865B-13-5 | 2 | 56.91 | 11.56 | 0.56 |
| 143-865B-14-5 | 2 | 59.05 | 11.54 | 0.49 |
| 143-865B-8-4 | 4 | 46.01 | 10.98 | 0.28 |
| 143-865B-8-6 | 3 | 47.34 | 11.70 | 0.16 |
| 143-865B-9-3 | 3 | 49.42 | 11.59 | 0.18 |
| 143-865B-9-6 | 3 | 51.35 | 12.80 | 0.11 |
| 199-1218A-11-1 | 2 | 25.50 | 12.39 | 1.09 |
| 199-1218A-14-5 | 2 | 27.50 | 11.62 | 0.74 |
| 199-1218A-16-3 | 2 | 28.50 | 14.65 | 0.04 |
| 199-1218A-18-1 | 2 | 29.50 | 12.89 | 0.16 |
| 199-1218A-26-2 | 4 | 37.50 | 11.19 | 0.40 |
| 199-1218A-26-5 | 1 | 38.50 | 9.84 | 0.00 |
| 199-1218A-27-2 | 1 | 39.50 | 9.97 | 0.00 |
| 199-1218A-28-1 | 1 | 40.50 | 10.14 | 0.00 |
| 199-1218A-29-1 | 4 | 41.50 | 10.70 | 0.33 |
| 199-1219A-17-7 | 1 | 34.50 | 10.58 | 0.00 |
| 199-1219A-18-5 | 2 | 36.07 | 10.46 | 0.49 |
| 199-1219A-19-1 | 2 | 37.00 | 10.99 | 0.41 |
| 199-1219A-19-5 | 2 | 38.25 | 13.11 | 0.04 |
| 199-1219A-20-2 | 2 | 39.05 | 11.31 | 0.07 |
| 199-1219A-21-1 | 2 | 40.16 | 10.45 | 0.45 |
| 199-1219A-21-8 | 3 | 41.04 | 10.75 | 0.36 |
| 199-1219A-23-4 | 3 | 43.14 | 11.66 | 0.30 |
| 199-1219A-24-2 | 2 | 44.34 | 11.81 | 0.18 |
| 199-1219A-24-4 | 2 | 45.31 | 12.22 | 0.31 |
| 199-1219A-24-6 | 4 | 46.34 | 11.42 | 0.25 |

continental shelves and slopes [7,37]. We conclude that diagenesis is unlikely to be a complicating factor for our samples.

The biostratigraphic age model used to date most of our samples was the same one used for both the $\delta^{18}O$ and $\delta^{13}C$ in benthic foraminifera and the $\delta^{34}S$ in marine barite (E. Thomas personal communication). As many of the sites used in the $\delta^{18}O$, $\delta^{13}C$, and $\delta^{34}S$ are the same as those we used for $\delta^{18}O_{SO4}$, the relative timing of the peaks should be well constrained. However, a different biostratigraphic age model was used for ODP sites 1218 or 1219, from which most of our samples between 45 and 30 Myr were extracted. Therefore, there could be error in the dating of some of the samples, which could explain some of the variability between barite extracted from different sites (Fig. 3).

### 4.2. $\delta^{34}S_{SO4}$ over the Cenozoic

Sulfur isotopes in marine sulfate place constraints on the behavior of the sulfur cycle over the Cenozoic (Fig. 4d, [30]. The constant values for $\delta^{34}S_{SO4}$ between 50 and 3 Ma suggest that pyrite burial rates remained constant over this interval. This implies that as sulfate reduction rates vary as a function of sea level, the percentage of sulfide which is reoxidized must also vary proportionally to keep the difference between these fluxes constant (i.e. the amount of sulfide sequestered as pyrite). Alternatively the fractionation associated with sulfate reduction ($\varepsilon_S$) shifts to compensate for changes in pyrite burial rates, yielding buried pyrite with, on average, a different sulfur isotopic signature. Neither explanation is particularly satisfactory; large sea level changes over the Cenozoic imply major disruptions to sulfur cycling in organic-rich sediments and the idea that changes occur in precisely to maintain a constant $\delta^{34}S_{SO4}$ seems unlikely.

We can test the buffering capacity of the $\delta^{34}S_{SO4}$ to fluctuations in pyrite burial rates, which is a function of the residence time of sulfur in the oceans (for $\delta^{34}S_{SO4}$ is $>10^7$ yr — for example see [46]). When pyrite burial rates are held constant for 15 Myr and then increase 50% for 15 Myr, then decrease 50% for 15 Myr, the $\delta^{34}S_{SO4}$ increases and decreases by 1‰ and 3‰. When pyrite burial rates fluctuate randomly between these two

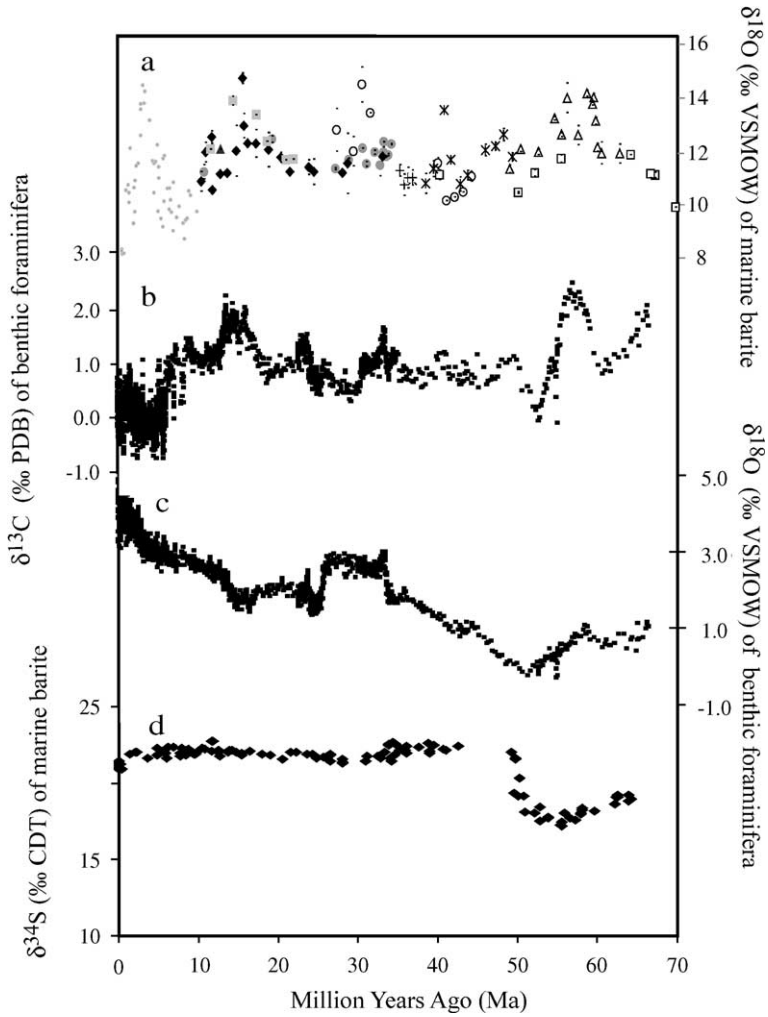


Fig. 4. (a) The $\delta^{18}O$ sulfate in marine barite (this work). See Fig. 3 for sites and legend. (b) The $\delta^{13}C$ measured in benthic foraminifera (Zachos et al., [45]). (c) The $\delta^{18}O$ measured in benthic foraminifera (Zachos et al., [45]). (d) The $\delta^{34}S$ of sulfate measured in marine barite (Paytan et al., [30]).

extremes every 400,000 yr, the $\delta^{34}S_{SO4}$ remains constant at 22‰. When pyrite burial rates fluctuate every 1.5 Myr (similar to the time scale of changes seen in the $\delta^{13}C$ of benthic foraminifera) the $\delta^{34}S_{SO4}$ changes by around 0.3‰, which is not large enough to be resolved in the $\delta^{34}S_{SO4}$ record of marine barite (Fig. 4d). This suggests that episodic fluctuations in pyrite burial rates are possible over the Cenozoic and not inconsistent with the sulfur isotope record. One explanation for the 5‰ increase in the $\delta^{34}S_{SO4}$ 50 Ma is a change in the average isotopic composition of pyrite buried through a change in the kinetic fractionation factor during sulfate reduction. This could occur from a reduction in the amount of pyrite formed during anaerobic methane oxidation (AMO—which produces heavier pyrite—[47]). This is temporally consistent with the eustatic sea level fall and reduction in shelf area from the drying out of the epicontinental seas where AMO was probably widespread. Two other possibilities for changing $\varepsilon_S$ are an increase in the amount of disproportionation (which produces isotopically lighter pyrite—[48]) or a decrease in the percentage of sulfur buried as organic sulfur versus pyrite (organic sulfur is isotopically heavier—J. Werne, personal communication).

### 4.3. Drivers of changes in the $\delta^{18}O_{SO4}$

The $\delta^{18}O_{SO4}$ can increase through several mechanisms. One is if the dominant reoxidation pathway switches to predominantly biological reoxidation or disproportionation reactions. These pathways proceed via sulfur intermediates, particularly sulfite ($SO_3^{2-}$) which can quickly equilibrate with water and become isotopically enriched. There may be other reoxidation

pathways which also proceed via intermediate valence state sulfur species and likely produce isotopically enriched sulfate. Biological sulfide reoxidation dominates in low-oxygen environments where sulfide oxidizing bacteria thrive.

Another way to increase the $\delta^{18}O_{SO4}$ is by increasing evaporite weathering. Most terrestrial evaporites have $\delta^{18}O_{SO4}$ between 13‰ and 18‰ [41] because they were deposited in earlier oceans when the $\delta^{18}O_{SO4}$ was heavier and because the $\delta^{18}O_{SO4}$ of gypsum is around 2‰ to 3‰ heavier than seawater sulfate [41]. If rivers were to reflect 100% evaporite weathering, which would also likely increase the riverine sulfate flux to the ocean, this could drive the ocean $\delta^{18}O_{SO4}$ heavier. If this occurred, however, we would expect to see an effect on sulfur isotopes in seawater sulfate as well. The $\delta^{34}S$ of terrestrial evaporites ranges from 20‰ to 25‰, only slightly heavier than seawater sulfate today, but rivers are the largest flux in the sulfur cycle for sulfur isotopes. Weathering evaporites, at the expense of weathering pyrite, will push the $\delta^{34}S$ of seawater sulfate higher.

A third way to increase the $\delta^{18}O_{SO4}$ is to permit sulfate to exchange isotopes with ocean water. If sulfate were in isotopic equilibrium with the ocean, it would be around 38‰ enriched over seawater [28]. We do not expect sulfate and water to equilibrate at current ocean temperature or pH [23]. It may be possible, however, that under certain chemical conditions the sulfur–oxygen bond in sulfate is weakened sufficiently to allow partial isotopic equilibration with water. This could be an effective way to make the seawater sulfate pool much heavier. It is unclear what those chemical conditions might be. Ocean pH has not varied enough to effect a change on sulfate–water equilibrium.

Another way to increase the $\delta^{18}O_{SO4}$ is through bacterial sulfate reduction, during which sulfate with light oxygen isotopes is preferentially reduced leaving a residual sulfate pool which is isotopically enriched. The highest rates of sulfate reduction occur in organic-rich sediments near the sediment–water interface (1 to 20 mol/m$^2$ yr) and this pool of isotopically enriched residual sulfate can return to the ocean through bioturbation. This has been observed in the modern ocean (e.g. [49]). Increased rates of bioturbation could accelerate this cycle. If rates of bioturbation were high enough to impact the global ocean $\delta^{18}O_{SO4}$, however, we might also expect an effect on the $\delta^{34}S$, which is also isotopically enriched in the residual pool.

A final way to increase the $\delta^{18}O_{SO4}$ is through the production and atmospheric oxidation of dimethyl sulfide ($H_3C–S–CH_3$, DMS). DMS is produced from the degradation of dimethylsulfonium propionate in marine algae, released as a gas, and oxidized in the atmosphere to sulfate [50]. This oxidation proceeds via $SO_2$, which equilibrates rapidly with water vapor, enriching the $SO_2$ by as much as 20‰ [22]. The $\delta^{18}O_{SO4}$ of precipitation sulfate is 15‰ to 25‰, and the majority of it lands on the oceans [22]. In the modern ocean the production and flux of DMS from the oceans is nearly one-third the flux of the riverine sulfate flux. This flux could become a large source of isotopically heavy sulfate to the ocean in times with more algal blooms than the modern.

There are fewer mechanisms to lower marine $\delta^{18}O_{SO4}$ than there are to raise it. The first is to increase pyrite weathering. This could occur through increased weathering of terrestrial pyrite or weathering of pyrite on exposed continental shelves during periods of low sea level. The problem with invoking weathering of pyrite to explain decreases in the $\delta^{18}O_{SO4}$ is that there should be a larger change in the $\delta^{34}S$ of seawater sulfate. Pyrite has a $\delta^{34}S$ between −10‰ and −70‰, much lighter than seawater sulfate, whereas the sulfate produced from oxidized pyrite has $\delta^{18}O_{SO4}$ between −10‰ and 0‰, depending on the $\delta^{18}O$ of the water in which it was oxidized. Therefore, major changes in pyrite weathering should be reflected in both the $\delta^{34}S$ and the $\delta^{18}O_{SO4}$ of marine sulfate.

Another way to decrease the $\delta^{18}O_{SO4}$ is to increase rates of direct sulfide oxidation. Direct sulfide oxidation is the oxidation of sulfide in oxic waters, and produces sulfate that has approximately the same isotopic composition of the water [28]. The oxygen in sulfate produced is largely derived from water because the electron acceptor at the sediment water interface is usually $Fe^{3+}$, not $O_2$ [28]. Direct sulfide oxidation occurs in several places in the modern ocean: sulfide produced in organic-rich sediments and diffuses or is bioturbated to the sediment–water interface is believed to be directly oxidized. This should also be the main oxidation pathway for any reduced sulfur compound that is produced in or arrives in the oxic water column, such as organic sulfur compounds (e.g. cysteine and methionine). Oxidation in the water column, however, takes place with $O_2$ as the electron acceptor. Incorporation of any $O_2$ into the final sulfate molecule should make it isotopically heavier, because the $\delta^{18}O$ of $O_2$ is +23‰ [51]. Experiments involving direct oxidation in water in the absence of $Fe^{3+}$ find that the sulfate is only 5‰ to 10‰ enriched over water because three of the oxygen atoms come from water [28].

To conclude, there are many drivers in the sulfur cycle that can increase or decrease the $\delta^{18}O_{SO4}$, however many of these changes will also affect the $\delta^{34}S_{SO4}$.

The only driver which can impact the $\delta^{18}O_{SO4}$ and not the $\delta^{34}S_{SO4}$ is changes in the isotopic fractionation during sulfide reoxidation. This flux is also the largest in the sulfur cycle and therefore is likely the driver of variability in the $\delta^{18}O_{SO4}$ over the Cenozoic.

### 4.4. Interpreting the Cenozoic $\delta^{18}O_{SO4}$ record

The $\delta^{18}O_{SO4}$ over the Cenozoic varies by 6‰ (Fig. 4a) in a pattern that seems cyclical with decreasing periodicity and increasing amplitude from the early Cenozoic to the modern. The $\delta^{18}O_{SO4}$ does not covary with the $\delta^{34}S$ over the Cenozoic (Fig. 4d). Therefore, the driver of temporal variability in $\delta^{18}O_{SO4}$ must be a change in the isotopic fractionation during sulfide reoxidation. Sulfate reduction and sulfide reoxidation occurs in organic-rich sediments; to change the dominant sulfide reoxidation pathway, environmental conditions in these sediments must change. The $\delta^{18}O_{SO4}$ record thus provides evidence for variations in the conditions within organic-rich sediments through the Cenozoic.

We can use our model to demonstrate why rivers cannot be driving variability in the $\delta^{18}O_{SO4}$ over the Cenozoic. Fig. 5a shows model results for a 10 Myr period where river input has been doubled for 3 Myr and the riverine sulfate reflects 100% evaporite weathering (15‰ $\delta^{18}O_{SO4}$ and 20‰ $\delta^{34}S$ for riverine sulfate). There is a much larger effect on sulfur isotopes than on oxygen isotopes. The $\delta^{18}O_{SO4}$ is able to quickly return to the pre-evaporite weathering levels, emphasizing the lower residence time for oxygen isotopes in marine sulfate. Sulfur isotopes lower gradually, and are still 3‰ enriched when the simulation ends. This emphasizes that changing the terrestrial weathering is an unlikely driver of changes in the $\delta^{18}O_{SO4}$ over the Cenozoic because we do not see variability in the $\delta^{34}S$. Fig. 5b shows model results for a 10 Myr simulation where the fractionation associated with reoxidation is increased by 5‰ for 3 Myr. This change in the reoxidation pathway

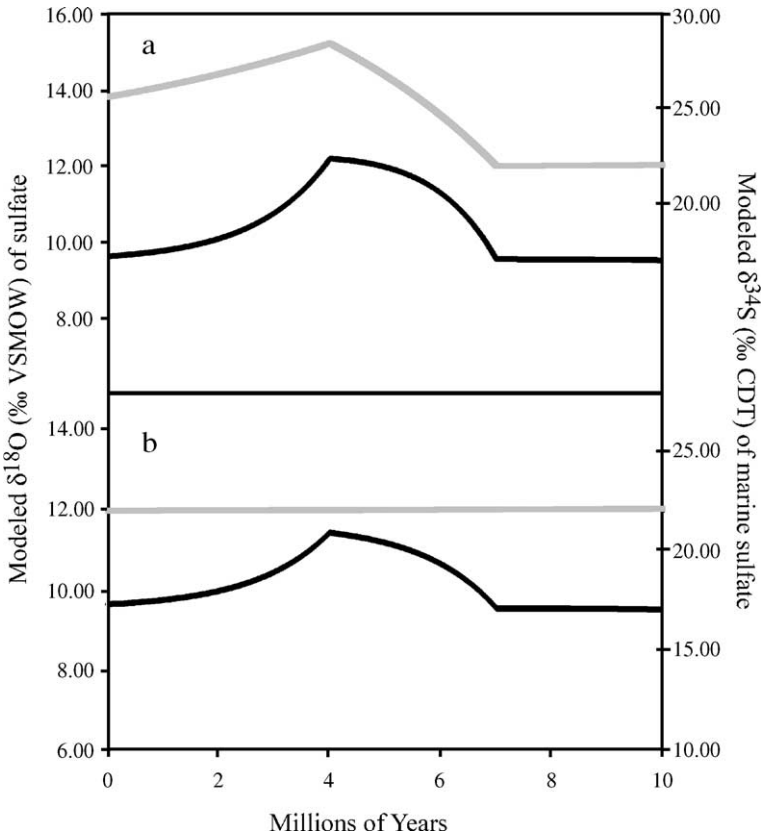


Fig. 5. Model results for potential drivers of variations in the oxygen isotopic composition of marine sulfate. (a) Model results for increased evaporite weathering. Black curve is oxygen isotopes, gray is sulfur isotopes. Evaporite weathering has a larger effect on sulfur isotopes than oxygen isotopes. (b) Model results for increasing the fractionation associated with sulfide reoxidation by 5‰. As expected, sulfur isotopes (gray) remain constant.

drives a 2‰ increase in the $\delta^{18}O_{SO4}$ and no change in the $\delta^{34}S$. This further emphasizes that changes in the reoxidation pathway are an efficient means to affect the $\delta^{18}O_{SO4}$ without impacting the $\delta^{34}S$.

Invoking changes in the isotopic fractionation associated with sulfide reoxidation over the Cenozoic implies that there may have been greater variability in the environments where organic matter is buried than previously thought. Variations in the $\delta^{13}C$ of benthic foraminifera provide a qualitative estimate of the net organic carbon burial through the Cenozoic. This net organic carbon burial flux, however, is less important to the sulfur cycle than the distribution of conditions under which it is buried. Sediments which have greater than 1% organic carbon will promote higher rates of sulfate reduction, but are also likely to be good environments for biological sulfur oxidation. On the other hand, sediments with less than 0.5% organic carbon will also promote high rates of sulfate reduction but the dominant reoxidation pathway will be direct oxidation. Switching between the aerial extent of these two types of environments of organic matter burial will dramatically impact how sulfur is processed and therefore the $\delta^{18}O_{SO4}$.

The $\delta^{18}O_{SO4}$ of sulfate throughout the ocean should be homogenous; the residence time of sulfate with respect to its oxygen isotopic composition is 1 Myr, which is over 1000 times the mixing time of the ocean. Therefore, it may be difficult to observe local variability in the $\delta^{18}O_{SO4}$ from the influence of different reoxidation pathways. In isolated basins which are not well mixed with the rest of the ocean, however, we do see isotopic variability. For example in Florida Bay, where organic carbon burial is high the $\delta^{18}O_{SO4}$ of the bottom water sulfate is isotopically heavy from biological sulfide oxidation [52]. Where Florida Bay connects with the rest of the ocean, the $\delta^{18}O_{SO4}$ of the water decreases to 9.8‰. Because of these local isotopic effects, care must be taken in choosing samples from paleoenvironments which were open to the ocean and likely to reflect a globally homogenous $\delta^{18}O_{SO4}$.

We therefore interpret variations in the $\delta^{18}O_{SO4}$ over the Cenozoic to reflect shifts in the aerial extent of anoxic, organic-rich sediments. At times when the $\delta^{18}O_{SO4}$ is low, organic carbon is being buried on the continental slope and in more oxic bottom waters, promoting direct sulfide oxidation as the dominant reoxidation pathway. When the $\delta^{18}O_{SO4}$ is high, organic carbon is dominantly deposited in shallower less oxic settings where biological sulfide oxidation dominates and isotopically heavy sulfate is produced. Estimating the aerial distribution of organic-rich sediments, we can use our model to calculate an integrated value for a steady state $\delta^{18}O_{SO4}$ for various oceans under different paleoceanographic conditions (Fig. 6). Our calculations suggest that for the Paleocene, when sea level was higher and there were extensive shallow continental seas, the steady state $\delta^{18}O_{SO4}$ should be around 15‰ (Fig. 6a), which compares well to our measured values. For the distribution of organic-rich sediments at the last glacial maximum (LGM) and in the modern ocean, the $\delta^{18}O_{SO4}$ should be 4‰ and 11‰, respectively (see Fig. 6b,c). The oceans have not been in steady state with respect to the sulfur cycle between the LGM and the modern, but the decline in the $\delta^{18}O_{SO4}$ over the past 3 Myr is due to the periodic shifting of organic matter burial from shelf environments during interglacials, to slope environments during glacial periods.

This interpretation can be applied throughout the Cenozoic. For example, from the Oligocene to the modern we interpret the $\delta^{18}O_{SO4}$ as a long decline punctuated by two transient increases. The long decline represents the increasing importance of organic carbon burial in deeper, slightly more oxygenated, sediments. The two positive excursions then would highlight periods of increased isotopic fractionation during reoxidation. The first excursion occurs 15 Ma at the Mid-Miocene climate optimum when carbon isotopes indicate increased organic matter burial [45]. This increased burial occurred in shallow sediments where biological sulfide oxidation would dominate, driving the $\delta^{18}O_{SO4}$ higher. The second positive excursion begins at the Miocene–Pliocene boundary, a time that is marked by a decrease in the pole-to-equator temperature gradient and increased nutrient supply to the oceans [53]. This boundary may have had a shift in environments where organic carbon is buried, as perhaps evidenced by the formation of the organic carbon rich late Miocene sapropels in the Mediterranean and Persian Gulf.

This interpretation represents a significant departure from the traditional view of the coupling between the carbon and sulfur cycles. We suggest that changes in sulfur cycling in organic-rich sediments, and therefore changes in pyrite burial and its isotopic composition, are influenced far more by changes in organic carbon content in sediments, rather than net organic carbon burial. Therefore the sulfur cycle may respond more to tectonic changes which influence basin geometry or nutrient supply to regions of the ocean rather than to changes in net carbon burial. For the $\delta^{18}O_{SO4}$ this may be a threshold effect: once organic carbon concentrations in sediments cross some threshold, the reoxidation

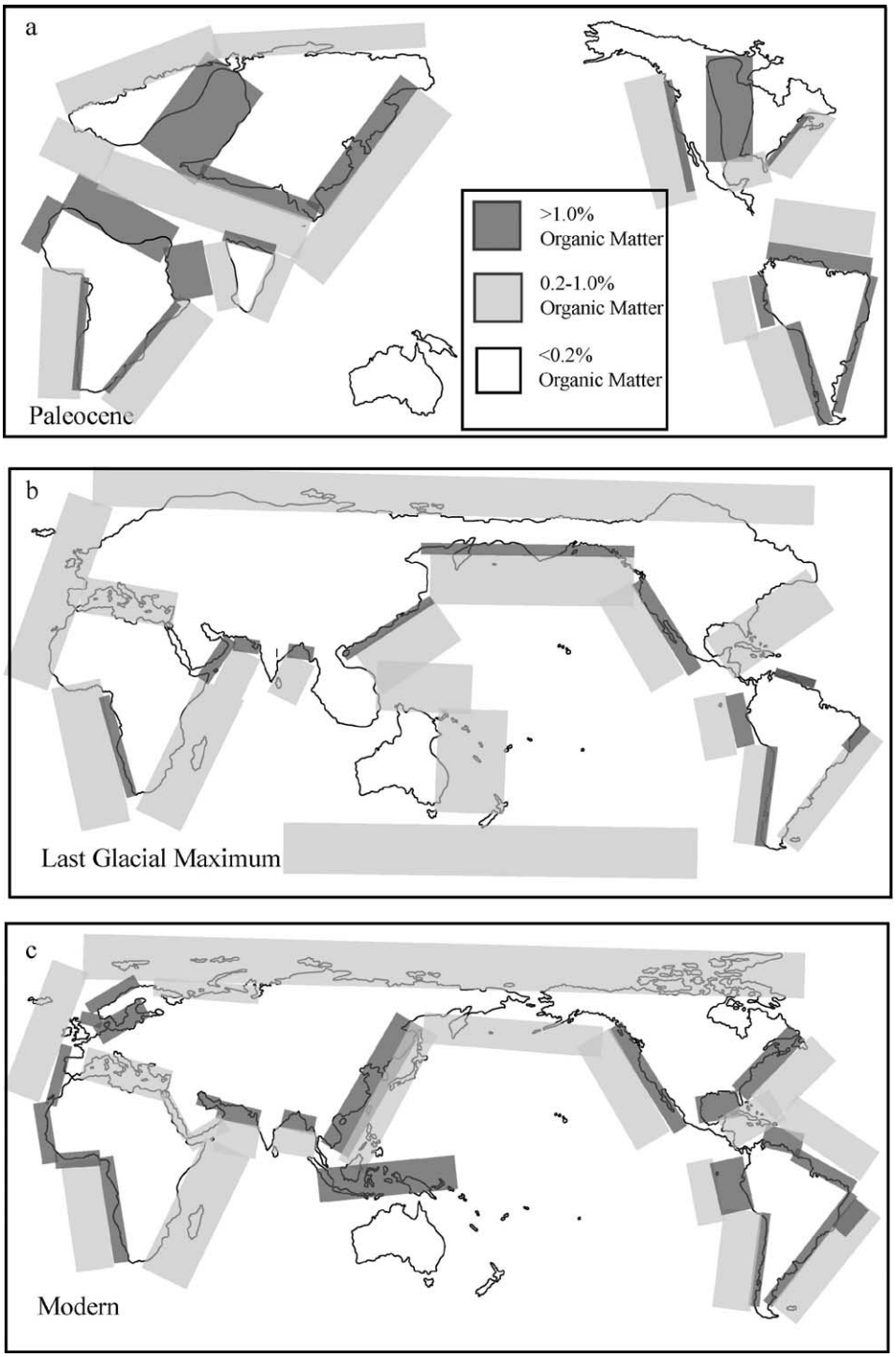


Fig. 6. Schematic drawings of qualitative changes in organic matter distribution at three times during the Cenozoic. (a) A hypothetical drawing of organic matter distribution during the Paleocene. Because more organic matter burial is concentrated in sediments with high organic content, the sulfur cycle is impacted and the calculated $\delta^{18}O_{SO4}$ is high. (b) A hypothetical drawing of organic matter burial during the Last Glacial Maximum. Because of low sea level, organic matter was buried in continental slope environments where the percentage of organic carbon was lower, impacting the sulfide reoxidation pathway and driving the $\delta^{18}O_{SO4}$ down. (c) Rough drawing of modern organic matter distribution (taken from [55,56]).

pathway switches from direct oxidation to biological oxidation and remains so even if organic carbon concentrations increase further.

An interesting question is whether this work may elucidate changes in marine sulfate concentrations over the Cenozoic. Our modeling suggests that increased area of continental shelves might have reduced sulfate concentrations in the Early Cenozoic, consistent with sulfate concentrations inferred from fluid inclusions [54]. However, the amplitude of the four excursions in the $\delta^{18}O_{SO4}$ over the Cenozoic is similar, which could imply that sulfate concentrations were more or less constant over the Cenozoic or that the forcing mechanism changed over time. In our model, however, sulfate concentrations can increase by up to 10 to 15 mM over the Cenozoic through the gradual weathering of exposed sulfur minerals due to lower sea level without impacting either the oxygen or sulfur isotopic composition of sulfate in the ocean. Those data and these modeling results suggest that sulfate concentrations were probably lower in the early Cenozoic.

## 5. Conclusions

The $\delta^{18}O_{SO4}$ measured in marine barite showed variability over the past 65 Myr, with four excursions of approximately 6‰. The $\delta^{18}O_{SO4}$ did not co-vary with the $\delta^{34}S_{SO4}$, indicating that the processes controlling the $\delta^{18}O_{SO4}$ were likely changes in the isotopic fractionation associated with the sulfide reoxidation pathway which do not impact sulfur isotopes. We suggest that the $\delta^{18}O_{SO4}$ is responding to changes in the environments where organic carbon is being buried, from more diffuse regions with 0.5% or less organic carbon to more concentrated areas with 1% or more. This emphasizes that the sulfur cycle is less sensitive to changes in net organic carbon burial than to changes in the dominant environments where this carbon is buried, which will affect not only the sulfide reoxidation pathway and thus $\delta^{18}O_{SO4}$ but potentially the rates of pyrite formation and its isotopic composition. The major change in sulfur isotopes 55 Ma probably reflected a change in the isotopic composition of reduced sulfur minerals. Sulfur isotopes may be buffered against rapid changes in pyrite burial rates, although sensitive to step changes in pyrite burial.

## Acknowledgements

We thank L. Kump and one anonymous reviewer for comments which greatly improved this manuscript. Help with much of the laboratory portion of this project was provided by G. Eischeid, L. Wolchok, C. Bergin, and F. Moore. This work was supported by NSF Grant OCE-0452329 to D.P. Schrag and a Schlanger Ocean Drilling Program Graduate Fellowship and a Department of Defense American Society for Engineering Education Graduate Fellowship to A.V. Turchyn.

## References

[1] C. Niewöhner, C. Hensen, S. Kasten, M. Zabel, Deep sulfate reduction completely mediated by anaerobic methane oxidation in sediments of the upwelling area off Namibia, Geochim. Cosmochim. Acta 62 (3) (1998) 455–464.
[2] S. Kasten, B.B. Jørgensen, Sulfate reduction in marine sediments, in: H.D. Schulz, M. Zabel (Eds.), Marine Geochemistry, 2000, pp. 263–275.
[3] S.T. Petsch, R.A. Berner, Coupling the geochemical cycles of C,P, Fe and S: the effect on atmospheric O-2 and the isotopic records of carbon and sulfur, Am. J. Sci. 298 (1998) 246–262.
[4] A.V. Turchyn, D.P. Schrag, Oxygen isotope constraints on the sulfur cycle over the last 10 million years, Science 303 (2004) 2004–2007.
[5] B.B. Jørgensen, Mineralization of organic matter in the sea bed—the role of sulfate reduction, Nature 296 (1982) 643–645.
[6] R.A. Berner, J.T. Westrich, Bioturbation and the early diagenesis of carbon and sulfur, Am. J. Sci. 285 (1985) 192–206.
[7] D.E. Canfield, Sulfate reduction in deep-sea sediments, Am. J. Sci. 291 (1991) 177–188.
[8] B. Thamdrup, H. Fossing, B.B. Jørgensen, Manganese, iron, and sulfur cycling in a coastal marine sediment, Aarhus Bay, Denmark, Geochim. Cosmochim. Acta 58 (23) (1994) 5115–5129.
[9] K.-M. Huang, S. Lin, The carbon–sulfide–iron relationship and sulfate reduction rate in the East China Sea continental shelf sediments, Geochem. J. 29 (1995) 301–315.
[10] W.S. Borowski, T.M. Hoehler, M.J. Alperin, N.M. Rodriguez, C.K. Paull, Significance of anaerobic methane oxidation in methane-rich sediments overlying the Blake Ridge gas hydrates, in: C.K. Paull, R. Matsumoto, P.J. Wallace, W.P. Dillon (Eds.), Proceedings of the Ocean Drilling Program, Scientific Results, vol. 164, 2000, pp. 87–99.
[11] S. Lin, J.W. Morse, Sulfate reduction and iron sulfide mineral formation in Gulf of Mexico anoxic sediments, Am. J. Sci. 291 (1991) 55–89.
[12] P. Aharon, B. Fu, Microbial sulfate reduction rates and sulfur and oxygen isotope fractionations at oil and gas seeps in deepwater Gulf of Mexico, Geochim. Cosmochim. Acta 64 (2) (2000) 233–246.
[13] B. Bolin, R.B. Cook, The Major Biogeochemical Cycles and Their Interactions, Wiley Publishers, 1983.
[14] J.C.G. Walker, Global geochemical cycles of carbon, sulfur, and oxygen, Mar. Geol. 70 (1986) 159–174.
[15] J.M. Edmond, C. Measures, R.M. McDuff, L.H. Chan, R. Collier, B. Grant, L.J. Gordon, J.B. Corliss, Ridge crest hydrothermal activity and the balances of the major and minor elements in the ocean: the Galapagos data, Earth Planet. Sci. Lett. 46 (1979) 1–18.

[16] R.E. McDuff, J.M. Edmond, On the fate of sulfate during hydrothermal circulation at mid-ocean ridges, Earth Planet. Sci. Lett. 57 (1982) 117–132.
[17] H. Strauss, Geological evolution from isotope proxy signals—sulfur, Chem. Geol. 161 (1999) 89–101.
[18] J.C. Alt, W.C. Shanks, Serpentinization of abyssal peridotites from the MARK area, Mid-Atlantic Ridge: sulfur geochemistry and reaction modeling, Geochim. Cosmochim. Acta 67 (2003) 641–653.
[19] H. Berresheim, W. Jaeschke, The contribution of volcanoes to the global atmospheric sulfur budget, J. Geophys. Res. 88 (C6) (1983) 3732–3740.
[20] R.E. Stoiber, S.N. Williams, B. Huebert, Annual contribution of sulfur-dioxide to the atmosphere by volcanoes, J. Volcan. Geotherm. Res. 33 (1987) 1–8.
[21] W.T. Holser, I.R. Kaplan, H. Sakai, I. Zak, Isotope geochemistry of oxygen in the sedimentary sulfate cycle, Chem. Geol. 25 (1980) 1–17.
[22] B.D. Holt, P.T. Cunningham, A.G. Engelkemeir, D.G. Graczyk, R. Kumar, Oxygen-18 study of nonaqueous-phase oxidation of sulfur dioxide, Atmos. Environ. 17 (1983) 625–632.
[23] R.M. Lloyd, Oxygen isotope behavior in sulfate–water system, J. Geophys. Res. 73 (1968) 6099–6110.
[24] H. Chiba, H. Sakai, Oxygen Isotope exchange-rate between dissolved sulfate and water at hydrothermal temperatures, Geochim. Cosmochim. Acta 49 (1985) 993–1000.
[25] P. Fritz, G.M. Basharmal, R.J. Drimmie, J. Ibsen, R.M. Qureshi, Oxygen isotope exchange between sulphate and water during bacterial reduction of sulphate, Chem. Geol. 79 (1989) 99–105.
[26] M.E. Böttcher, B. Thamdrup, T.W. Vennemann, Oxygen and sulfur isotope fractionation during anaerobic bacterial disproportionation of elemental sulfur, Geochim. Cosmochim. Acta 65 (10) (2001) 1601–1609.
[27] M.E. Böttcher, B. Thamdrup, Anaerobic sulfide oxidation and stable isotope fractionation associated with bacterial sulfur disproportionation in the presence of $MnO_2$, Geochim. Cosmochim. Acta 65 (10) (2001) 1573–1581.
[28] D.R. Van Stempvoort, H.R. Krouse, Controls of $\delta^{18}O$ in sulfate; review of experimental data and application to specific environments, Environmental Geochemistry of Sulfide Oxidation, American Chemical Society, 1994, pp. 446–480.
[29] A. Paytan, M. Kastner, E.E. Martin, J.D. MacDougall, T. Herbert, Marine barite as a monitor of seawater strontium isotope composition, Nature 366 (1993) 445–449.
[30] A. Paytan, M. Kastner, D. Campbell, M. Thiemens, Sulfur isotopic composition of Cenozoic seawater sulfate, Science 282 (1998) 1459–1462.
[31] A. Paytan, M. Kastner, D. Campbell, M. Thiemens, Seawater sulfur isotope fluctuations in the Cretaceous, Science 304 (2004) 1663–1665.
[32] R.S. Ganeshram, R. Francois, J. Commeau, S.L. Brown-Leger, An experimental investigation of Barite formation in seawater, Geochim. Cosmochim. Acta 67 (2003) 2599–2605.
[33] R.E. Bernstein, R.H. Byrne, J. Schijf, Acantharians: a missing link in the oceanic biogeochemistry of barium, Deep-Sea Res. 45 (1998) 491–505.
[34] J.D. Hopwood, S. Mann, A.J. Gooday, The crystallography and possible origin of barium sulphate in deep sea rhizopod protests (Xenophyophorea), J. Mar. Biol. Assoc. U.K. 77 (4) (1995) 969–987.
[35] J.K. Böhlke, S.J. Mroczkowski, T.B. Coplen, Oxygen isotopes in nitrate: new reference materials for $^{18}O$:$^{17}O$:$^{16}O$ measurements and observations on nitrate–water equilibration, Rapid Comm. Mass Spec. 17 (2003) 1835–1846.
[36] E. Berner, R.A. Berner, Global Environment: Water, Air, and Geochemical Cycles, Prentice Hall, 1996.
[37] S. D'Hondt, S. Rutherford, A.J. Spivack, Metabolic activity of subsurface life in deep-sea sediments, Science 295 (2002) 2067–2070.
[38] R.A. Berner, Burial of organic carbon and pyrite sulfur in the modern ocean: its geochemical and environmental significance, Am. J. Sci. 282 (1982) 451–473.
[39] K.L. Von Damm, Controls on the chemistry and temporal variability of seafloor hydrothermal fluids, in: S.E. Humphries, R.A. Zierenberg, L.S. Mullineaux, R.W. Thomson (Eds.), Seafloor hydrothermal systems: physical, chemical, biological, and geological interactions, AGU Monograph, vol. 91, pp. 222–247.
[40] F. Pawellek, F. Frauenstein, J. Veizer, Hydrochemistry and isotope geochemistry of the upper Danube River, Geochim. Cosmochim. Acta 66 (21) (2002) 3839–3854.
[41] G.E. Claypool, W.T. Holser, I.R. Kaplan, H. Sakai, I. Zak, The age curves of sulfur and oxygen isotopes in marine sulfate and their mutual interpretation, Chem. Geol. 28 (1980) 199–260.
[42] H.R. Krouse, B. Mayer, Sulphur and oxygen isotopes in sulphate, in: P.G. Cook, A.L. Herczeg (Eds.), Environmental Tracers in Subsurface Hydrology, 2000, pp. 195–231.
[43] J. Detmers, V. Bruchert, K.S. Habicht, J. Kuever, Diversity of sulfur isotope fractionations by sulfate-reducing prokaryotes, Appl. Environ. Microbiol. 67 (2) (2001) 888–894.
[44] R.T. Lowson, Aqueous oxidation of pyrite by molecular oxygen, Chem. Rev. 85 (1982) 461–497.
[45] J.C. Zachos, M. Pagani, L. Sloan, E. Thomas, K. Billups, Trends, rhythms, and aberrations in global climate 65 Ma to present, Science 292 (2001) 686–693.
[46] F.M. Richter, K.K. Turekian, Simple models for the geochemical response of the ocean to climatic and tectonic forcing, Earth Planet. Sci. Lett. 119 (1993) 121–131.
[47] B.B. Jørgensen, M.E. Böttcher, H. Lüschen, L.N. Neretin, I.I. Volkov, Anaerobic methane oxidation and a deep $H_2S$ sink generate isotopically heavy sulfides in Black Sea sediments, Geochim. Cosmochim. Acta 68 (9) (2004) 2095–2118.
[48] D.E. Canfield, B. Thamdrup, The production of S-34 depleted sulfide during bacterial disproportionation of elemental sulfur, Science 266 (1994) 1973–1975.
[49] R.C. Aller, N.E. Blair, Sulfur diagenesis and burial on the Amazon shelf: major control by physical sedimentation processes, Geo-Mar. Lett. 16 (1996) 3–10.
[50] M.D. Kumar, D.M. Shenoy, V.V.S.S. Sarma, M.D. George, M. Dandekar, Export fluxes of dimethylsulfoniopropionate and its breakdown gases at the air–sea interface, Geophys. Res. Lett. 29 (2002), doi:10.1029/2001GL013967.
[51] P. Kroopnick, H. Craig, Atmospheric oxygen—isotopic composition and solubility fractionation, Science 175 (1972) 54.
[52] T.C.W. Ku, L.M. Walter, M.L. Coleman, R.E. Blake, A.M. Martini, Coupling between sulfur recycling and syndepositional carbonate dissolution: evidence from oxygen and sulfur isotope composition of pore water sulfate, South Florida Platform, USA, Geochim. Cosmochim. Acta 63 (1999) 2529–2546.
[53] K.M. Grant, G.R. Dickens, Coupled productivity and carbon isotope records in the southwest Pacific Ocean during the late

Miocene–early Pliocene biogenic bloom, Palaeogeogr., Palaeoclimatol., Palaeoecol. 187 (2002) 61–82.
[54] J. Horita, H. Zimmerman, H.D. Holland, Chemical evolution of seawater during the Phanerozoic: implications from the record of marine evaporites, Geochim. Cosmochim. Acta 66 (21) (2002) 3733–3756.
[55] R.A. Berner, Burial of organic carbon and pyrite sulfur in the modern ocean: its geochemical and environmental significance, Am. J. Sci. 282 (1982) 451–473.
[56] S. Emerson, J.I. Hedges, Processes controlling the organic carbon content of open ocean sediments, Paleoceanography 3 (1988) 621–634.